Performance Analysis of Hybrid Peak to Average Power Ratio Reduction Techniques in 5G UFMC Systems

ALI F. ALMUTAIRI [ID], (Senior Member, IEEE), MISHAL AL-GHARABALLY, (Member, IEEE), AND APARNA KRISHNA

Electrical Engineering Department, College of Engineering and Petroleum, Kuwait University, Kuwait 13020, Kuwait

Corresponding author: Ali F. Almutairi (ali.almut@ku.edu.kw)

ABSTRACT The universal filtered multi-carrier (UFMC) technique has been proposed as a prominent waveform candidate for fifth generation (5G) communication techniques. However, UFMC systems exhibit a high peak-to-average power ratio (PAPR), which causes serious degradation in the performance of the system. Therefore, this paper puts forward an effective hybrid PAPR reduction method to reduce the high PAPR of the UFMC system. The proposed hybrid scheme consists of a combination of precoding and non-linear companding techniques (NLCTs). A comparative analysis of the performance of different precoding methods, NLCTs, and hybrid methods are investigated in terms of the cumulative distribution function of the PAPR and the bit error rate (BER). The simulation results show that the proposed hybrid UFMC system has better PAPR reduction performance compared to conventional NLC and precoded UFMC systems. Moreover, the BER analysis of the UFMC system verifies that the proposed hybrid technique shows better BER performance compared to conventional companding techniques.

INDEX TERMS Peak-to-average power ratio (PAPR), precoding techniques, non-linear companding techniques, hybrid PAPR reduction techniques, universal filtered multi-carrier (UFMC), 5G.

I. INTRODUCTION

Fifth Generation wireless networks have become an important research topic due to their potential applications in the wireless industry and in the evolution of new applications, such as the Internet of things (IoT), vehicular communications, and ultra-reliable and low-latency Communications (URLLC) [1], [2]. Compared to current 4G communication systems, 5G wireless technology must be able to handle not only an enormous number of applications but also a distinct category of users with various demands. The 4G systems are based on the cyclic prefix-orthogonal frequency division multiplexing (CP-OFDM) technique. CP-OFDM uses a cyclic prefix to eliminate inter-symbol-interference (ISI) and has high tolerance against multipath propagation and fading. However, due to the use of the cyclic prefix, CP-OFDM experiences high-spectrum efficiency loss. Moreover, the CP-OFDM spectrum has high out-of-band (OoB) side lobes, causing problems with reduced spectrum effi-

ciency when many pieces of user equipments are operating at one location. Due to these considerable drawbacks, OFDM is not considered an efficient technique for 5G communications.

Various types of waveforms have been proposed to deal with the new challenges that 5G networks are expected to handle. These waveforms, including filter-bank multicarrier (FBMC), generalized frequency division multiplexing (GFDM), filtered-OFDM (F-OFDM) and universal filtered multicarrier (UFMC), are more powerful than conventional OFDM because of their reduced spectral side-lobe levels [3]–[7]. In these new waveforms, UFMC is a novel multi-carrier modulation technique, that is currently being proposed as an attractive waveform candidate for next-generation wireless communication [8], [9]. In recent years, a great deal of research has been done to investigate the ability of UFMC to support advance applications for 5G communications systems [8]–[13]. A coordinated multi-point (CoMP) reception technique with UFMC (CoMP-UFMC) have been proposed in the presence of multiple CFOs [8]. Moreover, the new cyclic prefix (CP)

The associate editor coordinating the review of this manuscript and approving it for publication was Muhammad Khandaker.

based UFMC (CP-UFMC) system have been proposed to support interference-free one-tap equalization in the absence of transceiver imperfections. In [12], it has been shown that the CP UFMC is capable of suppressing the effects of interference as well as reducing the OoB power spectrum, and a new channel equalization algorithm is proposed to improve the system performance during non ideal conditions. In standard UFMC, the entire bandwidth is divided into a number of sub-bands, and each sub-band consists of a number of sub-carriers. UFMC then adopts a sub-band filtering approach in which each sub-band is filtered through pulse-shaping filters before transmission; therefore, the filter length can be reduced considerably compared to other 5G approaches [8], [10], [11]. Thus, UFMC is considered as the best choice for short-burst communication [8]. The sub-band filtering approach provides design flexibility and reduces ISI. It can also achieve better spectrum efficiency because it does not require the cycle prefix, leading to the reduction of OoB emission. Furthermore, due to the design flexibility of the UFMC system, it can accommodate the demands of individual users and service types by modifying the filter characteristics and system parameters. However, the high value of the PAPR is the major drawback of UFMC systems that affects the performance of power amplifiers used for the up-link transmissions.

Several techniques have been proposed to reduce PAPR, such as coding techniques, discrete fourier transform (DFT)-spreading techniques, precoding techniques, clipping techniques, selective mapping techniques, the partial transmit sequence techniques, and companding techniques [14]–[19]. Clipping is the simplest and most straightforward PAPR reduction approach that clips the amplitude of the signal to a fixed level. However, the clipping based PAPR reduction technique causes clipping noise and in-band and OoB interference, which results in performance degradation [20], [21]. Companding is another technique used to reduce PAPR. A simple, non-complex companding technique was proposed in [22] to reduce PAPR. The use of the above mentioned PAPR reduction techniques was originally proposed for OFDM and cannot be directly implemented in UFMC systems due to different frame structures.

However, there is some recent work on PAPR reduction in 5G systems [23]–[28]. In [23], a precoding-based method was proposed to reduce PAPR for UF-OFDM and F-OFDM modulation schemes. The proposed method transformed the F-OFDM signal to a single carrier signal and the UF-OFDM signal to a multicarrier signal with a smaller number of carriers and was therefore able to keep the spectral efficiency of the original system [23]. Later, a comparison of different types of clipping methods used to reduce PAPR was discussed in [24]. The authors proved that the deep clipping method reduced PAPR efficiently but showed very poor BER performance. A hybrid PAPR reduction scheme for UFMC using selective mapping and clipping was proposed in [25].

A. CONTRIBUTIONS

The focus of this work is on providing a detailed analysis of a hybrid PAPR reduction technique that is suitable for UFMC systems. The proposed PAPR reduction technique consists of a combination of the precoding and NLCTs. This combination reduces PAPR significantly and is proved to be one of the optimum methods to reduce PAPR in OFDM and FBMC systems [28]–[30]. This motivates us to investigate this method for a UFMC system to reduce PAPR. PAPR reduction using the precoding technique (also known as the pulse shaping technique) is a dynamic and flexible PAPR reduction technique. This method works with any kind of base-band modulation technique and can even reduce the PAPR up to the PAPR of a single carrier transmission technique [23]. Companding is an easy and less complex PAPR reduction technique. In this technique, the small signals are enlarged while compressing the large signals to increase the immunity of small signals from noise. We analyzed two different NLC methods, the Mu-Law companding technique, and the advanced rooting companding technique (ARCT), and compared their performance in terms of PAPR and BER.

B. PAPER ORGANIZATION

The reminder of this paper is organized as follows. Section II introduces the basic UFMC system model. Detailed explanations of the transmitter and receiver blocks are also provided. In Section III, a brief explanation of PAPR is provided. The proposed hybrid model to reduce the PAPR is explained in Section IV. A brief explanation of the various methods used for the analysis is also provided in this section. The simulation analysis and comparison of results are provided in Section V, and Section VI concludes the paper.

Notations: In this work, vectors are represented by bold capital and small letters, depending on whether they are time or frequency domains; matrices are represented by bold italic capital letters; and scalars are represented by normal small letters. The operators $C[.]$, $C^{-1}[.]$, $[.]^T$, $[.]^H$ and $E[.]$ denote companding, decompanding, transpose, Hermitian transpose and expectation, respectively. $sgn\{.\}$ represents the sign function, and $'*'$ represents the convolution operation. I_M represents the identity matrix of size M × M, and $j = \sqrt{-1}$. Variables n and k are the time index and the sub-carrier index, respectively.

II. UFMC SYSTEM ARCHITECTURE

The transceiver block diagram of a typical UFMC system is shown in Fig. 1. In contrast to the OFDM system, the UFMC system divides the entire band of sub-carriers (M) into a number of sub-bands (B), and then the data in each sub-band is processed by the IDFT and the sub-band filter in series. Finally, the filtered signals in all sub-bands are added together to generate the UFMC signal for transmission purposes.
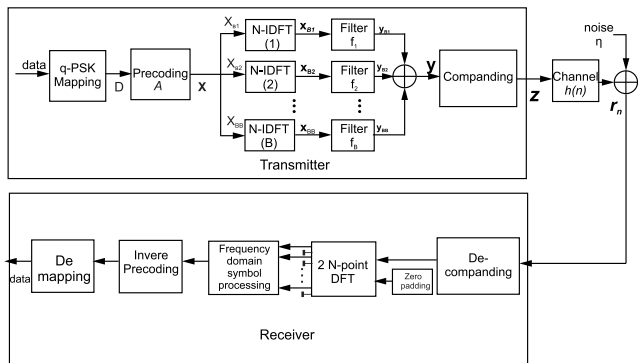
FIGURE 1. Block diagram of UFMC network.

A. TRANSMITTER

As illustrated in Fig. 1, the base-band modulation used will be $q - PSK$, where q represents the modulation size and the data symbols are applied to the modulation block. The output of the modulator can be represented as D, where $D = [d_0\ d_1 \cdots d_{M-1}]^T$, where d_j represents the modulated data with the sub-carrier index, $j = [0, 1, \cdots,$ M-1]. The modulated data vector D can then be multiplied with a precoding matrix A and can be represented as in (1):

$$\mathbf{X} = \mathbf{A}\,\mathbf{D}, \tag{1}$$

where A represents the precoding matrix of size M $\times$ M, as shown in (2). Equation (1) can be expanded in matrix form and is given in (3).

$$A = \begin{bmatrix} a_{00} & a_{01} & \cdots & a_{0(M-1)} \\ a_{10} & a_{11} & \cdots & a_{1(M-1)} \\ \vdots & \vdots & \ddots & \vdots \\ a_{(M-1)0} & a_{(M-1)1} & \cdots & a_{(M-1)(M-1)} \end{bmatrix} \tag{2}$$

$$\begin{bmatrix} X(0) \\ X(1) \\ \vdots \\ X(M-1) \end{bmatrix}$$

$$= \begin{bmatrix} a_{00} & \cdots & a_{0(M-1)} \\ a_{10} & \cdots & a_{1(M-1)} \\ \vdots & \ddots & \vdots \\ a_{(M-1)0} & \cdots & a_{(M-1)(M-1)} \end{bmatrix} \begin{bmatrix} d(0) \\ d(1) \\ \vdots \\ d(M-1) \end{bmatrix} \tag{3}$$

Using (3), the kth sub-carrier of X can then be written as (4), where $k = 0, 1, \cdots, \cdots, \cdots, M - 1$.

$$X(k) = \sum_{m=0}^{M-1} a(k, m)d(m) \tag{4}$$

The M $\times$ 1 precoded data vector $X = [X(0), X(1) \cdots, X(K), \cdots, X(M - 1)]^T$ is divided into B sub-bands, and each sub-band consists of M_B sub-carriers such that $M = BM_B$. The signal of each sub-band is applied to individual N-point inverse discrete fourier transforms (IDFTs) to get the time-domain signal, as shown in (5). However, before
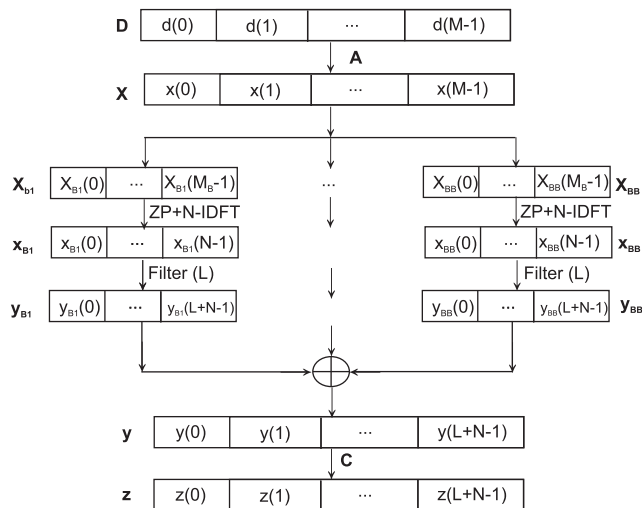

FIGURE 2. UFMC architecture.

doing the IDFT operation, each unoccupied frequency block will be zero padded to make a block of N symbols. Each zero padded symbol stream then passes through the N-point IDFT block to generate a time-domain vector $x_{Bi}(n)$.

$$x_{Bi}(n) = IDFT\,[\mathbf{X_{Bi}}] = \frac{1}{\sqrt{N}} \sum_{k=0}^{N-1} X_{Bi}e^{j2\pi nk/N} \tag{5}$$

The time-domain signals in (5) then pass through a Dolph–Chebyshev filter f_i of length L. The selection of filter length is an important factor because it will change the characteristics of the UFMC system, such as the OoB emissions, and thus its overall performance. The long filter length may lead to capacity reduction due to the overhead, and at the same time too short a filter length may also cause performance loss due to the multipath fading channel [31]. The resulting filtered signal is denoted by y_{Bi}, as represented in (6). Due to the linear convolution operation, the filter output will have a length equal to $N+L-1$. After that, these time-domain output signals from different sub-bands will combine to generate UFMC waveform **y**, given by (7).

$$\mathbf{y_{Bi}} = \mathbf{x_{Bi}} * \mathbf{f_i} \tag{6}$$

$$\mathbf{y} = \sum_{i=0}^{B-1} \mathbf{y_{Bi}} \tag{7}$$

Finally, a companding transform acts on the generated precoded UFMC signal vector **y** to reduce the PAPR, as shown in (8).

$$z(n) = C[y(n)] \tag{8}$$

B. RECEIVER

Assume that perfect channel state information is available at the receiver. Therefore, the received signal can be represented as (9), where, $h(n)$, $\eta(n)$ represent the channel response and the additive white Gaussian noise (AWGN), respectively.

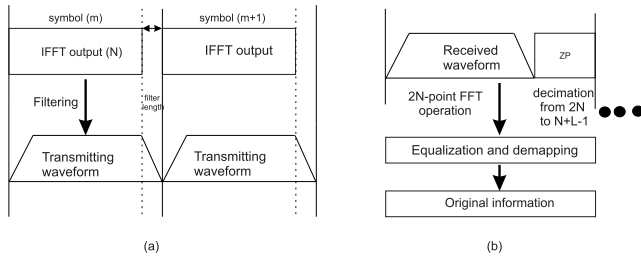$$r(n) = \mathbf{h(n)} * \mathbf{z(n)} + \eta(n), \tag{9}$$

FIGURE 3. UFMC symbol property. (a) Transmitter. (b) Receiver.

$$v(n) = C^{-1}[r(n)] \qquad (10)$$

After passing through the channel, the received signal at the receiver will be decompanded, as shown in (10). The decompanded signal has $(N + L - 1)$ samples and requires a 2N point FFT to demodulate it. This is done by padding the companded signal with $(N - L + 1)$ zeros to make the overall length of the signal 2N. Then, the $2N$-point DFT is performed on the signal as shown in (11).

$$\mathbf{S(k)} = \frac{1}{\sqrt{2N}} \sum_{v=0}^{N+L-2} v(l) \, e^{-j2\pi lk/2N} \qquad (11)$$

It is worth to mention that the 2N-point DFT operation slightly enhances the statistical properties of the noise vector. After the 2N-point DFT operation, the signal is down sampled by a factor of 2. The down-sampling procedure preserve all the signals with data symbols and discard symbols with interferences. Later, the down-sampled signal is processed with frequency-domain symbol processing procedure to eliminate the effect of filter distortion. Zero-forcing method is utilized for equalization. Finally, the equalized symbols are de-mapped using $q-PSK$ modulation to generate the original information. The property of UFMC symbol at the transmitter and receiver can be represented as shown in Fig. 3.

III. PEAK TO AVERAGE POWER RATIO OF UFMC SYSTEM
A UFMC multicarrier system has B sub-bands, and each sub-band consists of a large number of modulated signals in each sub-carrier. This will introduce a large PAPR value after the addition procedure at the transmitter end [23]. The PAPR is the ratio of the maximum power of a transmitted signal divided by the average power of the same signal. PAPR in UFMC can be represented as in (12).

$$PAPR = \frac{max(|z(n)|^2)}{E[|z(n)|^2]} \qquad (12)$$

CCDF is used to analyze the efficiency of a PAPR reduction technique. The high PAPR level in the transmitter leads to the performance degradation of power amplifiers and increases the OoB radiation. Therefore, to increase the efficiency of the UFMC system and to reduce the PAPR, we propose a hybrid PAPR reduction technique.

IV. PAPR REDUCTION TECHNIQUES
In this section, various techniques used to improve the performance of UFMC signals are discussed. A combination

strategy consisting of precoding and NLC techniques is proposed to reduce the PAPR of a transmitted UFMC signal. In the proposed approach, the precoding algorithm is applied to a q-PSK modulated signal. The compression operation is then performed after the sub-band filtering operation, as shown in Fig. 1.

A. PRECODING TECHNIQUES
The precoding based PAPR reduction technique is an efficient and flexible approach to reduce the PAPR in a multicarrier system. In the precoding technique, each of the modulated data symbols is first multiplied by a precoding matrix ($\mathbf{A}$) of size M × M before the IDFT operation to reduce the PAPR. In this work, three types of precoding matrices are used to analyze the performance of precoding in a UFMC system.

1) DISCRETE HARTLEY TRANSFORM
A discrete Hartley transform (DHT) is a linear real-valued orthogonal transform. In DHT, N real numbers $(x_0, x_1, \ldots, x_{N-1})$ are transformed into N-real numbers $(X_0, X_1, \ldots, X_{N-1})$. The N point DHT/IDHT can be implemented as in (13) and (14): [16]

$$X_k = \sum_{n=0}^{N-1} x_n cas(2\pi nk/N), \qquad (13)$$

$$x_n = 1/N \sum_{n=0}^{N-1} X_k cas(2\pi nk/N), \qquad (14)$$

where $k = 0, 1, 2, \cdots, N - 1$, and $cas\theta = \cos\theta + \sin\theta$ represent the precoding matrix kernel. It is clear from (13) and (14) that both forward and inverse Hartley transforms are identical and are invertible transforms.

2) DISCRETE SINE TRANSFORM
The discrete sine transform (DST) of a sequence of length N can be written as in (15): [28]

$$X_K = \sum_{n=0}^{N-1} x_n \sin\left(\frac{\pi nm}{N+1}\right), \qquad (15)$$

where, $a_{mn} = \sin(\pi mn/N+1)$ represents the precoded matrix element, k, m, and n are integers from 0 to $N - 1$.

3) DISCRETE FOURIER TRANSFORM
A discrete fourier transfrom (DFT) of a sequence of length N can be written as in (16):

$$X_K = \sum_{n=0}^{N-1} x_n e^{-j2\pi nk/N}, \qquad (16)$$

and the IDFT can be written as in (17):

$$x_n = \frac{1}{N} \sum_{n=0}^{N-1} X_K e^{j2\pi nk/N} \qquad (17)$$

$a_{mn} = e^{-j2\pi mn/N}$ represents the precoded matrix element, and m, and n are integers from 0 to $N - 1$.

B. DFT BASED PRECODED UFMC SYSTEM

As shown in Fig. 1, a precoding based PAPR reduction technique is proposed to reduce the high PAPR of UFMC systems. At the transmitter, the vector of M-PSK symbols D is first multiplied by a precoding matrix A to generate the precoded vector, as shown in (4). As a result of the precoding procedure, optimum detection of the symbols at the receiver may be difficult. Thus, to reduce the complexity of the precoding procedure, a proper selection of the elements of the precoding matrix A is required. The precoding matrix A must satisfy the following conditions:

- The precoding matrix must be an orthogonal matrix. That is, $AA^H = I_M$.
- If DFT precoding technique is used, then all the entries of the precoding matrix can be represented as shown below [32].

$$a_{im} = a_{i0} e^{\frac{-2\pi im}{M}} \qquad (18)$$

The UFMC output signal can be represented as shown in (7), which given by (19) in expanded form.

$$y(u) = \sum_{i=1}^{B} \sum_{n=0}^{N-1} x_{Bi}(n) f_i(u - m) \qquad (19)$$

By using (4), (5) and (18), $x_{Bi}(n)$ can be represented as,

$$x_{Bi}(n) = \sum_{l=(i-1)M_B}^{iM_B-1} \sum_{m=0}^{M-1} a_{n0} d_m e^{\frac{-2j\pi ml}{M}} e^{\frac{2j\pi nl}{N}} \qquad (20)$$

$$= IDFT \left[DFT \left[d_{mn} \right] \right] \qquad (21)$$

DFT and IDFT operations will effectively cancel each other and hence (19) can be written as,

$$y(u) = \sum_{i=1}^{B} \sum_{n=0}^{N-1} d_i(n) f_i(u - m) \qquad (22)$$

From (22), it is clear that the DFT-precoded UFMC signal can be represented as the summation of B single carrier signals at the output of pulse shaping filter and hence, the UFMC system becomes equivalent to a single carrier system [23]. Thus, the PAPR of UFMC system is reduced without increasing the system complexity. Meanwhile if DHT precoding technique is considered, then (20) can be represented as shown in (23),

$$x_{Bi}(n) = \sum_{l=(i-1)M_B}^{iM_B-1} \sum_{m=0}^{M-1} a_{n0} d_m cas \left(\frac{2\pi ml}{M} \right) e^{\frac{2j\pi nl}{N}} \qquad (23)$$

$$x_{Bi}(n) = \sum_{l=(i-1)M_B}^{iM_B-1} \sum_{m=0}^{M-1} \left[d_{mn} \left(\cos \left(\frac{2\pi ml}{M} \right) + \sin \left(\frac{2\pi ml}{M} \right) \right) \right]$$
$$\times e^{\frac{2j\pi nl}{N}} \qquad (24)$$

Thus, the output of pulse shaping filter may be given by,

$$y(u) = \sum_{i=1}^{B} \left(\sum_{l=(i-1)M_B}^{iM_B-1} \sum_{m=0}^{M-1} d_{mn} \left(\cos \left(\frac{2\pi ml}{M} \right) + \sin \left(\frac{2\pi ml}{M} \right) \right) \right.$$
$$\left. \times e^{\frac{2j\pi nl}{N}} \right) f_i(u - m) \qquad (25)$$

C. NON-LINEAR COMPANDING TECHNIQUE

The non-linear companding technique (NLCT) is an efficient method to reduce the PAPR in multicarrier systems. NLCT is a type of clipping approach that provides better PAPR reduction with less implementation complexity. It compress the original UFMC signal at the transmitter end by using a monotonic function, and an inverse procedure is performed at the receiver end before the signal is fed to any other operation. The companding technique expands the low amplitude signals while constricting the amplitude of high amplitude signals. Different types of NLCTs are described in the literature, such as the Mu-Law and A-Law companding method, exponential companding, error-function companding, tanh companding, and ARCT [22], [33], [34].

1) MU-LAW COMPANDING TECHNIQUE

The Mu-Law companding is an NLCT that is similar to the clipping approach. However, it offers very good PAPR reduction and better BER performance compared to normal clipping methods. The Mu-Law companding technique compresses the original signal using monotonically increasing functions, and this operation is performed on the transmitted signal after the sub-band filtering operation. Thus, the signal can be easily recovered at the receiver using the inverse transform function. The companding function applied to the end of the transmitter side can be expressed as in (26):

$$C(y[n]) = sgn(y[n]) \frac{\ln(1 + \mu y[n])}{\ln(1 + \mu)}, \qquad (26)$$

where μ represents the compression ratio, and as μ increases there will be more compression for higher amplitude of the transmitted signal. The inverse companding operation can be represented as in (27):

$$C^{-1}(r[n]) = sgn(r[n]) \frac{1}{\mu} \left((1 + \mu)^{|r[n]|} - 1 \right) \qquad (27)$$

2) ADVANCED ROOTING COMPANDING TECHNIQUE

The ARCT is an NLCT used to reduce the PAPR. It is a modified version of the square rooting companding method. The modified rooting companding technique can be represented as in (28):

$$z(n) = C(y(n)) = |y(n)|^R sgn(y(n)), \qquad (28)$$

where R is a mean companding parameter, the value of which lies between 0.1 and 0.9 and the *sgn* function is used to maintain the phase of the UFMC signal. The ARCT affects the amplitude of the signal, but leaves the phase value unchanged. The value of R determines the rate of change of the signal amplitude. Later, at the receiver end, the rooting decompanding technique is applied to recover the compressed signal and can be represented as in (29).

$$C^{-1}(r(n)) = |r(n)|^{1/R} sgn(r(n)) \qquad (29)$$

TABLE 1. Simulation parameters of UFMC system.

Size of FFT (N)	1024
Total number of sub-carriers (M)	384
Modulation method (q)	QPSK & 16-PSK
Number of sub-bands (B)	32
The number of sub-carriers in each sub-band (M_B)	12
Sidelobe attenuation	40dB
Window	Dolph–Chebyshev
Filter length or CP length	43
Channel	AWGN

FIGURE 4. CCDF of the standard and different precoded UFMC signals without companding.

D. PROPOSED HYBRID PAPR REDUCTION TECHNIQUE

In this section, the proposed hybrid PAPR reduction technique that combines NLCTs with the precoding technique to reduce the PAPR of UFMC system is analyzed. Precoding methods and NLCTs are used independently to reduce the PAPR of any multicarrier systems. In this study, these two methods are combined to attain a further reduction in the PAPR of a UFMC system. The advantages of both precoding and companding techniques have been exploited in the hybrid technique. The companding transform introduces some distortion and increases receiver noise, while precoding has no effect on the receiver data rate.

In the next section, we compare the effect of these PAPR-reduction methods on UFMC signals and compare the results of each method using computer simulations.

V. RESULTS AND DISCUSSIONS

To evaluate and compare the performance of the proposed hybrid scheme, a MATLAB simulation is performed, assuming an AWGN channel and using randomly generated data bits with QPSK and 16-PSK modulation techniques. To verify the performance of the proposed hybrid technique, simulation results of PAPR and BER plots are presented. The performance of UFMC has been evaluated in accordance with 3GPP LTE-10 MHz radio frame structure with total number of sub-carriers equals to 1024 and a subcarrier spacing of 15KHz. Total number of occupied sub-carriers is 600 which is divided into number of sub-bands and each sub-band is composed by 12 sub-carriers. The UFMC parameters derived from LTE System parameters are summarized in Table. 1.

A. PAPR ANALYSIS FOR PRECODING, MU-LAW, AND ARCT TECHNIQUES

In this section, we investigate different PAPR reduction methods independently. Fig. 4 shows the CCDF comparison of different precoding schemes used to reduce the PAPR in a UFMC system for different modulation orders. For the PAPR analysis using the precoding technique, three different precoding approaches–DFT precoded based
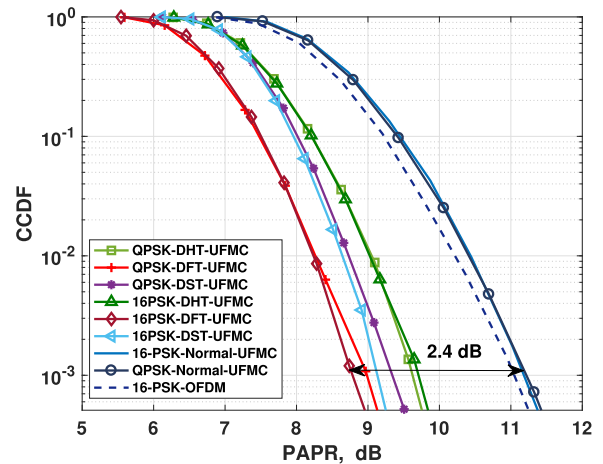
UFMC (DFT-UFMC), DHT precoded UFMC (DHT-UFMC) and DST precoded UFMC (DST-UFMC)–are used. Initially, a set of random data is generated and modulated using QPSK and 16-PSK methods. Later, the modulated data is precoded using three different precoding matrices. From Fig. 4, it is clear that the DFT-UFMC system achieves a PAPR gain of 2.4 dB compared to a standard-UFMC system at CCDF = 10^{-3}.

Therefore, it can be seen that the PAPR performance of the DFT-UFMC system outperform the standard or other precoding-based UFMC systems as mentioned in Section IV-B. Thus, it is proved that the analytical analysis matches the simulation results in the case of precoded UFMC system. Hence, adding a DFT precoding block to the conventional UFMC modulation scheme improves the PAPR of the UFMC system without increasing the system complexity.

B. PAPR ANALYSIS FOR PRECODING, MU-LAW, AND ARCT TECHNIQUES

Later, the PAPR of the UFMC system is analyzed as a function of the PAPR for different values of compression factors. Fig. 5 shows the CCDF of the UFMC system using the Mu-Law companding technique for 16-PSK modulation. It can be observed from Fig. 5 that when the value of the compression coefficients (μ) of Mu-Law increases, the PAPR decreases.

Fig. 6 shows the CCDF characteristics of the proposed ARCT for 16-PSK modulation. It is clear from Fig. 6 that, when the value of R decreases the PAPR also decreases. This means, the parameter R has a positive influence on the PAPR characteristics.

Based on the above analysis, it can be observed that both the precoding and NLCTs improve the PAPR performance of our UFMC system compared to a normal UFMC system. However, a hybrid PAPR reduction procedure is proposed to further reduce the PAPR. As explained previously, DFT-UFMC provides better PAPR performance compared to other precoded UFMC systems. Therefore, we use only the
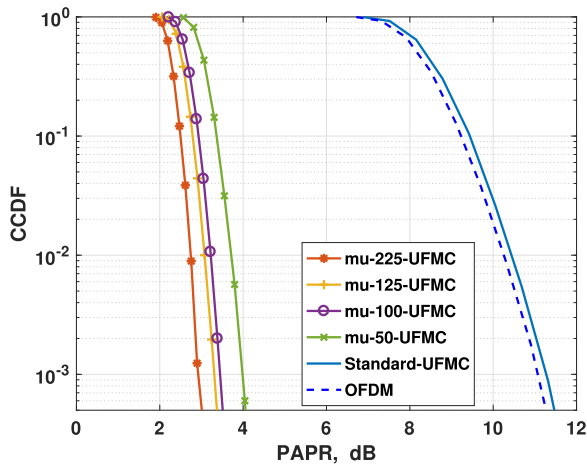
FIGURE 5. CCDF of the standard and Mu-Law companded UFMC signals using 16-PSK modulation.
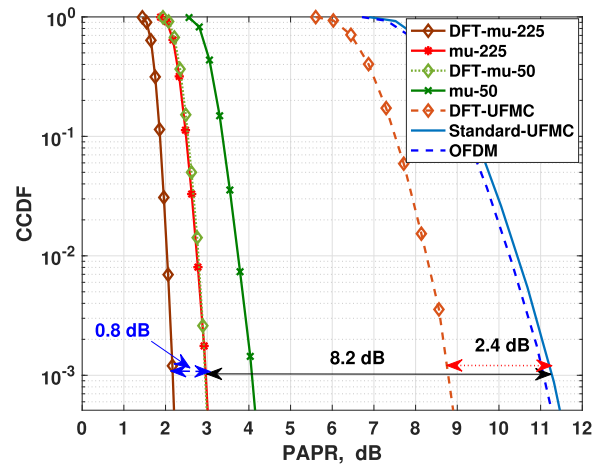

FIGURE 7. Comparison of the PAPR of the hybrid Mu-Law companding technique with the standard and Mu-Law companded UFMC signals using the 16-PSK modulation technique.
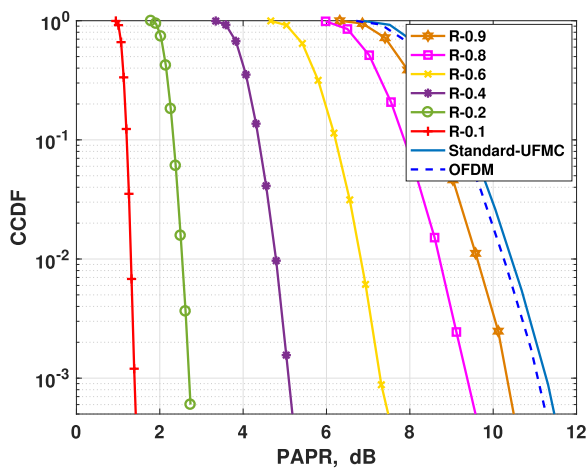

FIGURE 6. CCDF of the standard and ARCT UFMC signals using 16-PSK modulation.
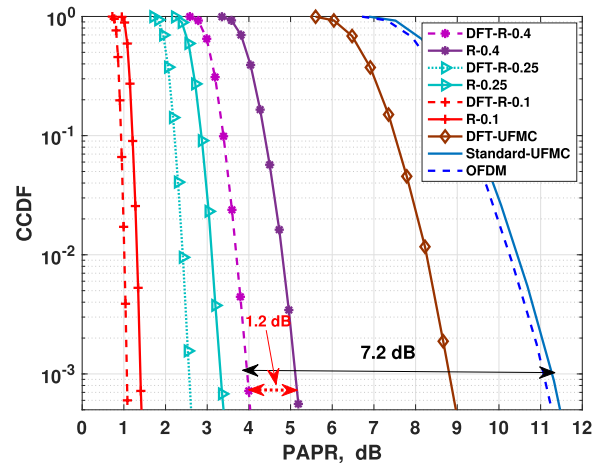

FIGURE 8. Comparison of the PAPR of the hybrid ARCT with the standrad and ARCT UFMC signals using the 16-PSK modulation technique.

DFT precoding method for the proposed hybrid precoding based PAPR reduction technique.

C. PROPOSED DFT-NLC TECHNIQUE

In this section, the effect of the hybrid PAPR reduction technique on the UFMC system using DFT-UFMC with the NLCT is investigated. Fig. 7 shows the results of the comparison of the CCDF of the PAPR of the standard-UFMC system and the proposed hybrid DFT-mu-μ ($\mu = 225, 50$) system. The figure also shows the plots of the DFT precoding and the Mu-Law companding UFMC system without DFT precoding.

Fig. 8 shows the comparison of hybrid ARCT with the standard and ARCT UFMC signals using the 16-PSK modulation technique. Initially, the DFT precoding technique improves the PAPR without affecting the BER characteristics. Then, the ARCT further reduces the PAPR value, as shown in the figure. A detailed analysis of the results of the hybrid methods are available in the Discussion section.

D. PERFORMANCE OF THE BER RATE OF THE PROPOSED TECHNIQUES

Fig. 9 shows the comparison of the BER performance of the precoded-UFMC system with the standard UFMC for the 16-PSK modulation technique. As it is clear from this figure, the precoding has no effect on the BER performance of UFMC system in an AWGN channel. Fig. 10 and 11 show the BER comparison of UFMC system using the precoded Mu-Law companding technique and the precoded ARCT, respectively. It is clear from Fig. 10 that the BER of the Mu-Law companding transform increases with an increase in the compression coefficient. This is because, the Mu-Law companding technique enlarges only small signals and therefore increases the average power of the UFMC system. This is the most undesired effect of the Mu-Law companding technique, which involves the requisite expansion of the compressed signal at the receiver, a process that amplifies receiver noise. It is clear from Fig. 11 that the proposed ARCT provides the best bit error characteristics compared to the Mu-Law technique at 10^{-3} BER (10^{-3} is the minimum
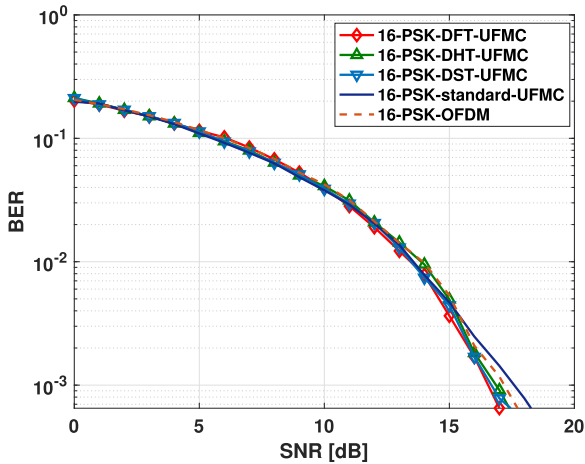
FIGURE 9. Comparison of the BER of the precoding technique using 16-PSK modulation.

FIGURE 11. Comparison of the BER of the hybrid ARCT with the standard and ARCT UFMC signals using 16-PSK modulation.
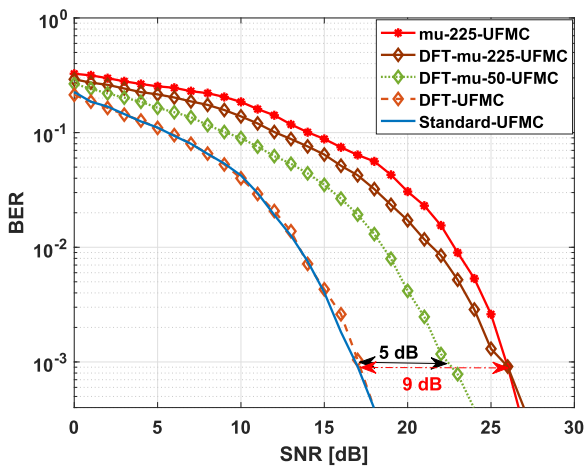

FIGURE 10. Comparison of the BER of the hybrid Mu-Law companding transforms with the standard and Mu-Law companded UFMC using 16-PSK modulation.

FIGURE 12. Comparison of the BER of the hybrid UFMC system with OFDM for different modulation schemes.

BER required for voice services). Fig. 12 shows the effect of modulation on BER characteristics. The analysis shows that both hybrid-NLCTs have better BER performance with QPSK modulation compared to a 16-PSK modulation scheme.

E. DISCUSSION

The hybrid precoding based NLCTs provide an improvement in PAPR with better BER characteristics compared to NLCTs without precoding and the traditional precoding technique. The following conclusions can be made, when comparing the proposed hybrid methods with a standard-UFMC system without a PAPR reduction approach.
- Performance of the precoding and NLC techniques: The precoding based PAPR reduction technique improves the CCDF of the PAPR and has no observable effect on its BER characteristics on the AWGN channel. However, the NLC-based PAPR-reduction technique improves the CCDF of the PAPR significantly but degrades the BER characteristics. When compared to the standard-UFMC system, the DFT-UFMC, Mu-Law ($\mu = 225$), and
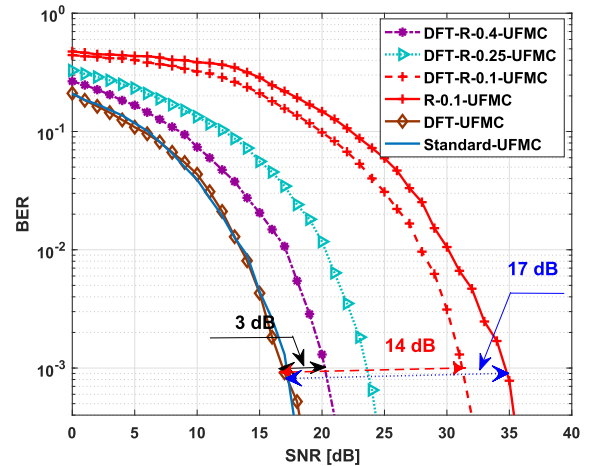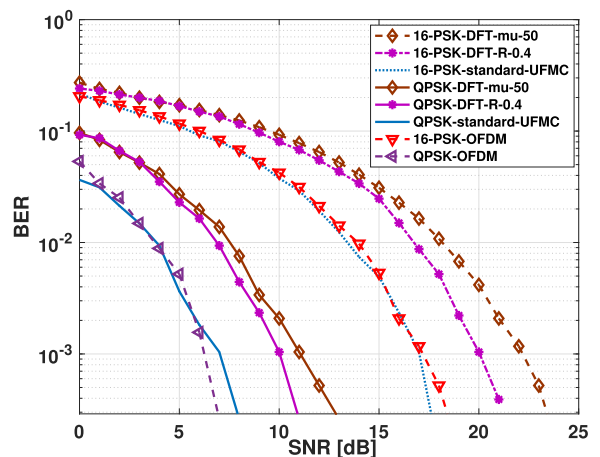
ARCT ($R = 0.1$) techniques achieve a PAPR gain of 2.4 dB, 8.2 dB, and 10 dB, respectively at CCDF= 10^{-3}. However, for the Mu-Law ($\mu = 225$) and ARCT ($R = 0.1$) techniques, the BER shows a degradation of 9 dB and 15 dB, respectively at BER = 10^{-3}. This means that, by using NLCT there is a trade-off between PAPR performance and BER characteristics.
- DFT-Mu-Law companding technique: The best PAPR performance with the hybrid Mu-Law companding technique is obtained at DFT-mu-225. However, the BER performance deteriorates by almost 9 dB at BER= 10^{-3} (from Fig. 10). Therefore, to achieve better PAPR and BER performance, we chose an appropriate μ value (DFT-mu-50). Then the proposed hybrid system shows an improvement in the CCDF of the PAPR of 8.2 dB, while the signal-to-noise (SNR) degradation is about 5 dB compared to the standard-UFMC. This means, there is an improvement in the BER of about 4 dB compared to DFT-mu-225. Moreover, this hybrid method has the same PAPR characteristics and a better SNR than Mu-Law companding without precoding ($mu - 225$).

- DFT-ARCT: The best enhancement in the CCDF of the PAPR is at DFT-R-0.1, and the improvement is 10.2 dB at CCDF = 10^{-3}. However, the SNR shows a degradation of about 14 dB compared to the standard-UFMC system. Therefore, to achieve better PAPR and BER performance, the value of R is chosen to be $-R = 0.4$. From Fig. 11 it is clear that, DFT$-R-0.4$ provides an improvement in the CCDF of the PAPR of 7.2 dB, while degradation of the SNR at BER = 10^{-3} is only 3 dB compared to standard-UFMC.

- The proposed hybrid ARCT method is proved to be an efficient method for reducing the PAPR in the UFMC system with better BER characteristics than Hybrid Mu-Law companding technique.

VI. CONCLUSION

In this paper, a novel hybrid PAPR reduction technique is proposed to reduce the PAPR of a UFMC system. A comparative analysis between two precoded NLCTs such as DFT-Mu-Law and DFT-ARCT, is implemented. The analysis proved that the hybrid technique imporoves PAPR reduction compared to a normal UFMC system. We also provide a comparative analysis between the precoding method, the Mu-Law technique, and the advanced rooting companding technique. Based on the analysis, DFT-ARCT is considered to be the most efficient in reducing PAPR compared to the Mu-Law and precoding techniques. A detailed comparison of the BER of the proposed hybrid system is also presented. The analysis prove that the precoded UFMC method preserves the BER performance of the standard UFMC system on the AWGN channel. However, the traditional NLCT affects the BER characteristics. The hybrid PAPR reduction techniques improves the BER characteristics of NLCTs. Simulation results indicated that the proposed hybrid ARCT can achieve better PAPR reduction with lower computational complexity and better BER performance compared to the hybrid Mu-Law technique. In the future, a modified PAPR reduction technique needs to be analyzed to improve both the PAPR and BER characteristics of UFMC systems on a frequency selective channel.

REFERENCES

[1] I. F. Akyildiz, S. Nie, S.-C. Lin, and M. Chandrasekaran, "5G roadmap: 10 key enabling technologies," *Comput. Netw.*, vol. 106, pp. 17–48, Sep. 2016.

[2] *IMT Vision–Framework and Overall Objectives of the Future Development of IMT for 2020 and Beyond*, Standard ITU-Rec. M.2083-0, 2015.

[3] F. Schaich and T. Wild, "Waveform contenders for 5G—OFDM vs. FBMC vs. UFMC," in *Proc. 6th Int. Symp. Commun. Control Signal Process. (ISCCSP)*, May 2014, pp. 457–460.

[4] P. Banelli, S. Buzzi, G. Colavolpe, A. Modenini, F. Rusek, and A. Ugolini, "Modulation formats and waveforms for 5G networks: Who will be the heir of OFDM?: An overview of alternative modulation schemes for improved spectral efficiency," *IEEE Signal Process. Mag.*, vol. 31, no. 6, pp. 80–93, Nov. 2014.

[5] Y. Liu *et al.*, "Waveform design for 5G networks: Analysis and comparison," *IEEE Access*, vol. 5, pp. 19282–19292, 2017.

[6] Y. Cai, Z. Qin, F. Cui, G. Y. Li, and J. A. McCann. (2017). "Modulation and multiple access for 5G networks." [Online]. Available: https://arxiv.org/abs/1702.07673

[7] R. Gerzaguet *et al.*, "The 5G candidate waveform race: A comparison of complexity and performance," *EURASIP J. Wireless Commun. Netw.*, vol. 1, p. 13, Jan. 2017.

[8] V. Vakilian, T. Wild, F. Schaich, S. T. Brink, and J. Frigon, "Universal-filtered multi-carrier technique for wireless systems beyond LTE," in *Proc. IEEE Globecom Workshops (GC Wkshps)*, Dec. 2013, pp. 223–228.

[9] T. Wild, F. Schaich, and Y. Chen, "5G air interface design based on universal filtered (UF-)OFDM," in *Proc. 19th Int. Conf. Digit. Signal Process.*, Aug. 2014, pp. 699–704.

[10] Y. Chen, F. Schaich, and T. Wild, "Multiple access and waveforms for 5G: IDMA and universal filtered multi-carrier," in *Proc. IEEE 79th Veh. Technol. Conf. (VTC Spring)*, May 2014, pp. 1–5.

[11] F. Schaich, T. Wild, and Y. Chen, "Waveform contenders for 5G-suitability for short packet and low latency transmissions," in *Proc. IEEE 79th Veh. Technol. Conf. (VTC Spring)*, May 2014, pp. 1–5.

[12] L. Zhang, P. Xiao, and A. Quddus, "Cyclic prefix-based universal filtered multicarrier system and performance analysis," *IEEE Signal Process. Lett.*, vol. 23, no. 9, pp. 1197–1201, Sep. 2016.

[13] C. Goztepe and G. K. Kurt, "The impact of out of band emissions: A measurement based performance comparison of UF-OFDM and CP-OFDM," *Phys. Commun.*, vol. 33, pp. 78–89, Apr. 2019. [Online]. Available: http://www.sciencedirect.com/science/article/pii/S1874490718303902

[14] R. van Nee and A. de Wild, "Reducing the peak-to-average power ratio of OFDM," in *Proc. 48th IEEE Veh. Technol. Conf. Pathway Global Wireless Revolution*, vol. 3, May 1998, pp. 2072–2076.

[15] S. A. Aburakhia, E. F. Badran, and D. A. E. Mohamed, "Linear Companding transform for the reduction of peak-to-average power ratio of OFDM signals," *IEEE Trans. Broadcast.*, vol. 55, no. 1, pp. 155–160, Mar. 2009.

[16] I. Baig and V. Jeoti, "PAPR analysis of DHT-precoded OFDM system for M-QAM," in *Proc. Int. Conf. Intell. Adv. Syst.*, Jun. 2010, pp. 1–4.

[17] V. Tabatabavakili and A. Zahedi, "Reduction in peak to average power ratio of OFDM signals using a new continuous linear companding transform," in *Proc. 5th Int. Symp. Telecommun.*, Dec. 2010, pp. 426–430.

[18] J. Mountassir, A. Isar, and T. Mountassir, "Precoding techniques in OFDM systems for PAPR reduction," in *Proc. 16th IEEE Medit. Electrotech. Conf.*, Mar. 2012, pp. 728–731.

[19] W. Wang, M. Hu, Y. Li, and H. Zhang, "A low-complexity tone injection scheme based on distortion signals for PAPR reduction in OFDM systems," *IEEE Trans. Broadcast.*, vol. 62, no. 4, pp. 948–956, Dec. 2016.

[20] X. Li and L. J. Cimini, "Effects of clipping and filtering on the performance of OFDM," in *Proc. IEEE 47th Veh. Technol. Conf. Technol. Motion*, vol. 3, May 1997, pp. 1634–1638.

[21] L. Yao, J. He, and X. Xu, "Analysis and comparison of two clipping methods in PAPR reduction for OFDM system," in *Proc. 5th Int. Conf. BioMed. Eng. Inform.*, Oct. 2012, pp. 1435–1438.

[22] X. Wang, T. T. Tjhung, and C. S. Ng, "Reduction of peak-to-average power ratio of OFDM system using a companding technique," *IEEE Trans. Broadcast.*, vol. 45, no. 3, pp. 303–307, Sep. 1999.

[23] M. B. Mabrouk, M. Chafii, Y. Louet, and F. Bader, "A precoding-based PAPR reduction technique for UF-OFDM and filtered-OFDM modulations in 5G systems," in *Proc. 23th Eur. Wireless Conf.*, May 2017, pp. 1–6.

[24] M. N. Tipán , J. Cáceres, M. N. Jiménez, I. N. Cano, and G. Arévalo, "Comparison of clipping techniques for PAPR reduction in UFMC systems," in *Proc. IEEE 9th Latin-Amer. Conf. Commun. (LATINCOM)*, Nov. 2017, pp. 1–4.

[25] P. Rani, S. Baghla, and H. Monga, "Hybrid PAPR reduction scheme for universal filter multi-carrier modulation in next generation wireless systems," *Adv. Syst. Sci. Appl.*, vol. 17, no. 4, pp. 22–33, 2017.

[26] W. Rong, J. Cai, and X. Yu, "Low-complexity PTS PAPR reduction scheme for UFMC systems," *Cluster Comput.*, vol. 20, no. 4, pp. 3427–3440, Dec. 2017.

[27] S. K. Bandari, V. M. Vakamulla, and A. Drosopoulos, "Novel hybrid PAPR reduction schemes for the MGFDM system," *Phys. Commun.*, vol. 31, pp. 69–78, Dec. 2018.

[28] I. Shaheen, A. Zekry, F. Newagy, and R. Ibrahim, "PAPR reduction for FBMC/OQAM using hybrid scheme of different Precoding transform and mu-law companding," *Int. J. Eng. Technol.*, vol. 6, no. 4, pp. 154–162, 2017.

[29] I. A. Shaheen, A. Zekry, F. Newagy, and R. Ibrahim, "PAPR reduction of FBMC/OQAM systems based on combination of DST Precoding and A-law nonlinear companding technique," in *Proc. Int. Conf. Promising Electron. Technol. (ICPET)*, Oct. 2017, pp. 38–42.

[30] C.-Y. Hsu and H.-C. Liao, "PAPR reduction using the combination of precoding and Mu-Law companding techniques for OFDM systems," in *Proc. IEEE 11th Int. Conf. Signal Process.*, vol. 1, Oct. 2012, pp. 1–4.

[31] J. Wen, J. Hua, W. Lu, Y. Zhang, and D. Wang, "Design of waveform shaping filter in the UFMC system," *IEEE Access*, vol. 6, pp. 32300–32309, 2018.

[32] S. B. Slimane, "Reducing the peak-to-average power ratio of OFDM signals through precoding," *IEEE Trans. Veh. Technol.*, vol. 56, no. 2, pp. 686–695, Mar. 2007.

[33] V. N. Sonawane and S. V. Khobragade, "Comparative analysis between A-law and-law companding technique for PAPR reduction in OFDM," *Int. J. Adv. Res. Comput. Commun. Eng.*, vol. 2.5, pp. 2210–2214, May 2013.

[34] I. A. Shaheen, A. Zekry, F. Newagy, and R. Ibrahim, "Modified square rooting companding technique to reduced PAPR for FBMC/OQAM," in *Proc. Palestinian Int. Conf. Inf. Commun. Technol. (PICICT)*, May 2017, pp. 66–70.

MISHAL AL-GHARABALLY was born in Kuwait, in 1976. He received the B.S. degree in electrical engineering from Kuwait University, in 1998, and the M.S. and Ph.D. degrees in electrical engineering from the University of California at San Diego, San Diego, in 2004 and 2007, respectively. Since 2007, he has been an Assistant Professor with the Electrical Engineering Department, Kuwait University. He is currently serving as the Vice Dean of admission and registration. His research interests include communications theory, wireless communications, signal processing, and channel coding.

ALI F. ALMUTAIRI (S'91–M'00–SM'07) received the B.S. degree in electrical engineering from the University of South Florida, Tampa, FL, USA, in 1993, and the M.S. and Ph.D. degrees in electrical engineering from the University of Florida, Gainesville, FL, USA, in 1995 and 2000, respectively. He served as the Vice Dean for academic affairs with the College of Engineering and Petroleum, Kuwait University, from 2016 to 2018. He served as the Chairperson for the Electrical Engineering Department, Kuwait University, from 2007 to 2011, and served as the Graduate Program Director of the Electrical Engineering Department, Kuwait University, from 2015 to 2016. He is currently an Associate Professor with the Electrical Engineering Department, and the Dean of admission and registration with Kuwait University. His current research interests include multiuser detection, wireless networks, antenna design, and current and future cellular networks performance issues. He is a member of other professional societies. He served/serving as an Associate Editor and a Reviewer for many technical publications. In 1993, he received a full scholarship from Kuwait University to pursue his graduate studies.

APARNA KRISHNA received the B.Tech. degree in electronics and communication engineering from Calicut University, Kerala, India, the M.E. degree in communication systems from Anna University, Chennai, India, in 2008, and the Ph.D. degree in electrical engineering from Qatar University, Doha, Qatar, in 2018. She has been a Lecturer with SBCE, Kerala, India, since 2009. From 2011 to 2013, she was a Research Assistant with the Department of Electrical Engineering, Qatar University, where she worked on application of statistical electromagnetics on harsh environments. From 2013 to 2016, she was a Teaching Assistant with the Electrical Engineering Department, Qatar University. She is currently a Research Associate with the Electrical Engineering Department, Kuwait University, Kuwait. Her research interests include the analysis and design of microstrip antennas, statistical electromagnetics, and broad area of 5G wireless communication systems.

. . .